Supporting Information

Hierarchical hollow $MnTe_2/CoTe_2$ composite nanospheres assembled from porous nanosheets: Synergistic structural engineering for high-performance hybrid supercapacitors

Akbar Mohammadi Zardkhoshoui[1]*, Erfan Behzadi,[2] Mohammad Ali Saghafizadeh,[2] and Saied Saeed Hosseiny Davarani[2]*

[1]Department of Chemical Technologies, Iranian Research Organization for Science and Technology (IROST), Tehran 3313193685, Iran.

[2]Department of Chemistry, Shahid Beheshti University, G. C., 1983963113, Evin, Tehran, Iran.

Corresponding authors: *[1]Tel: +98 21 56276283; Fax: +98 21 56276265; E-mail: A_mohammadi@irost.ir (A. Mohammadi Zardkhoshoui) and *[2]Tel: +98 21 22431661; Fax: +98 21 22431661; E-mail: ss-hosseiny@sbu.ac.ir (S.S.H. Davarani).

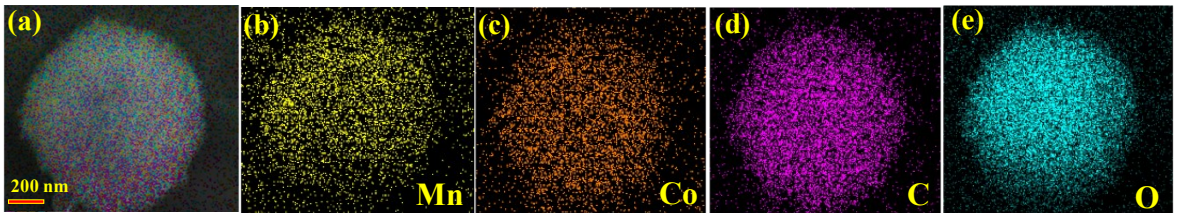

Fig. S1 FESEM mapping images of the MnCo-LDH.

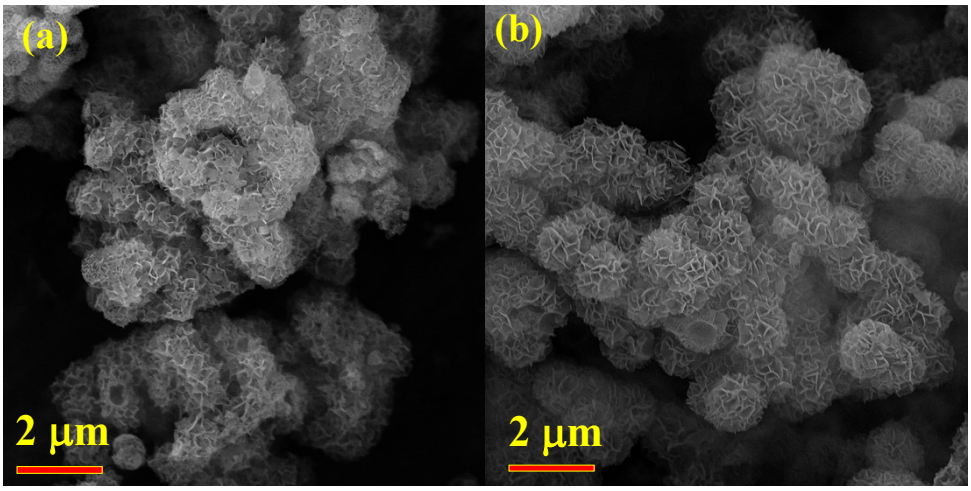

Fig. S2 (a) FESEM image of the $MnTe_2$, (a) FESEM image of the $CoTe_2$

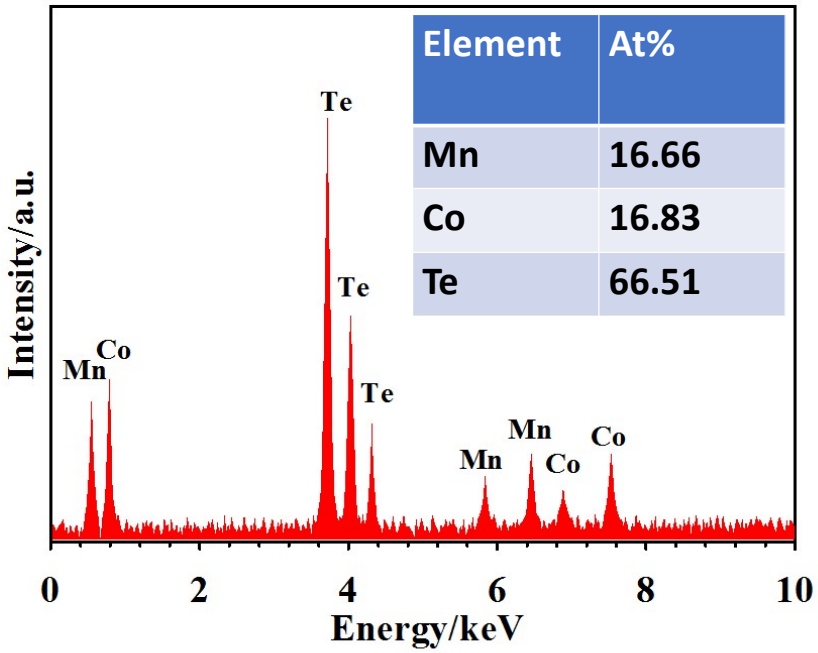

Fig. S3 EDS pattern of the MCT-500.

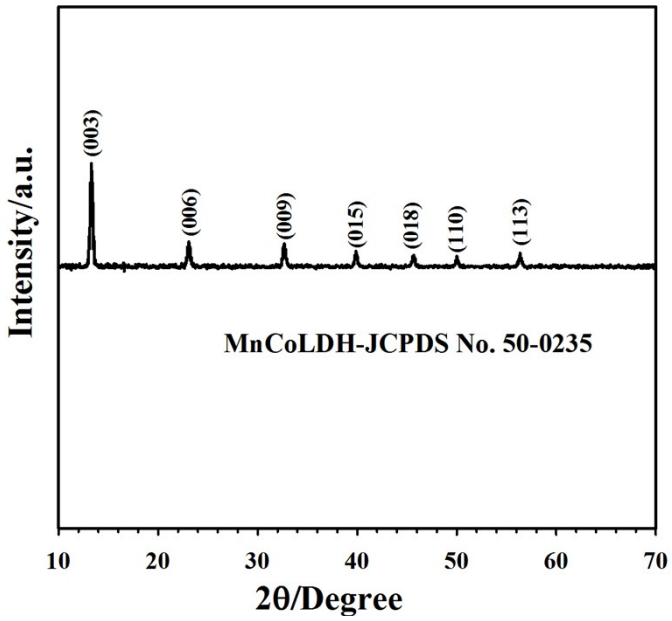

Fig. S4 XRD pattern of the MnCo-LDH.

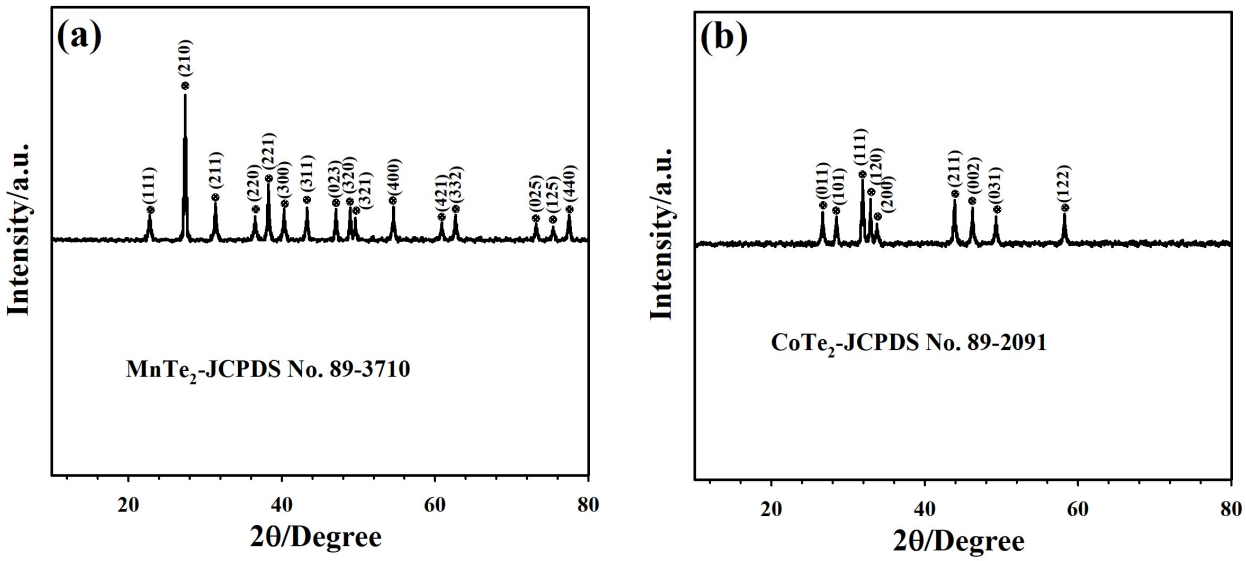

Fig. S5 (a) XRD pattern of the $MnTe_2$, (b) (a) XRD pattern of the $CoTe_2$.

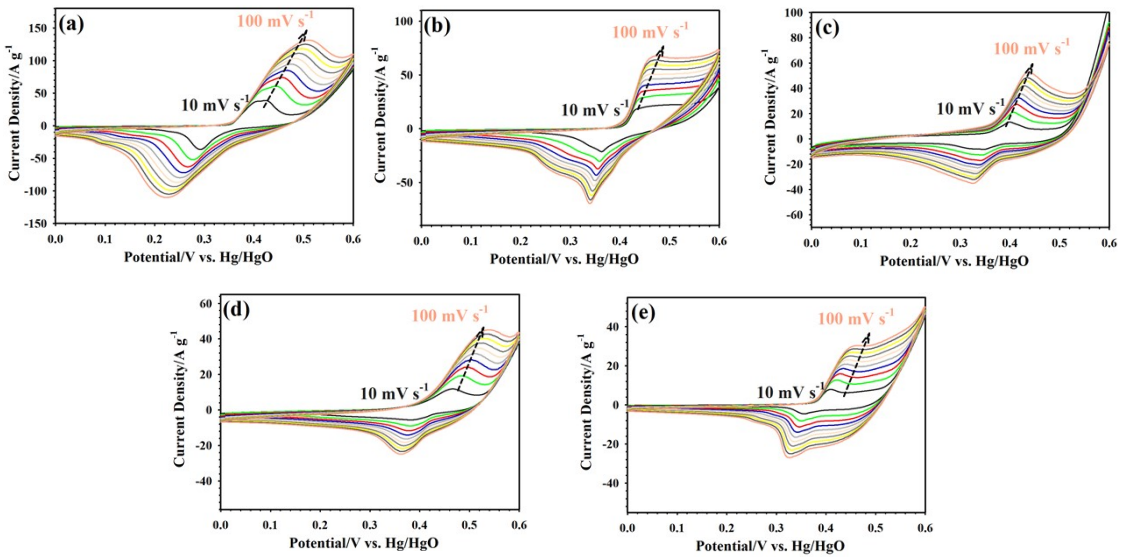

Fig. S6 (a) CV curves of the MCT-300 from 10 to 100 mV s^{-1}, (b) CV curves of the MCT-150 from 10 to 100 mV s^{-1}, (c) CV curves of the MnCo-LDH from 10 to 100 mV s^{-1}, (d) CV curves of the $CoTe_2$ from 10 to 100 mV s^{-1}, (e) CV curves of the $MnTe_2$ from 10 to 100 mV s^{-1}.

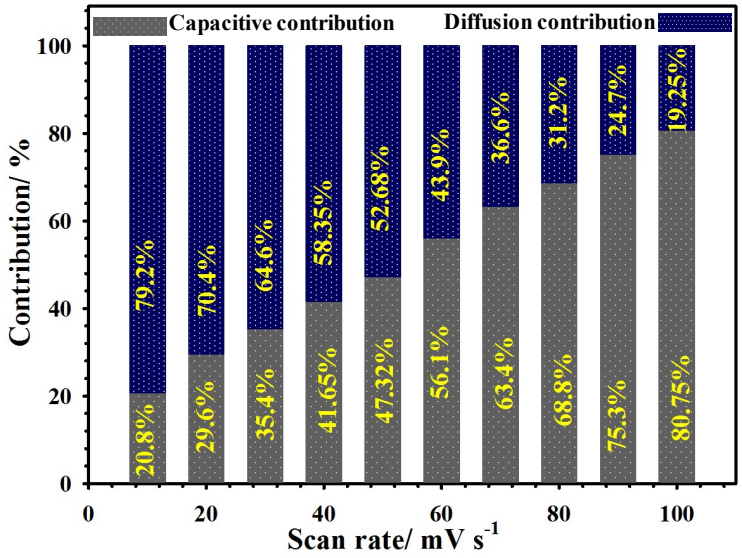

Fig. S7 Relative contribution of the capacitive and diffusion-controlled charge storage at various sweep speeds for MCT-500 based-electrode.

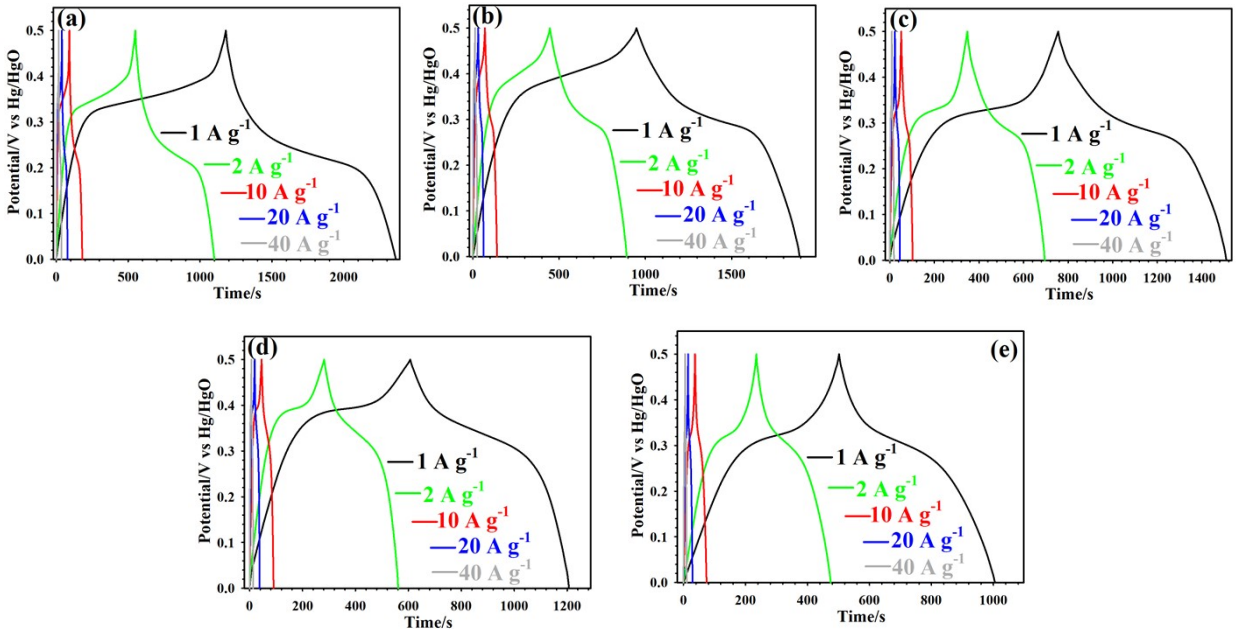

Fig. S8 (a) GCD curves of the MCT-300 from 1 to 40 A g^{-1}, (b) GCD curves of the MCT-150 from 1 to 40 A g^{-1}, (c) GCD curves of the MnCo-LDH from 1 to 40 A g^{-1}, (d) GCD curves of the $CoTe_2$ from 1 to 40 A g^{-1}, (e) GCD curves of the $MnTe_2$ from 1 to 40 A g^{-1}.

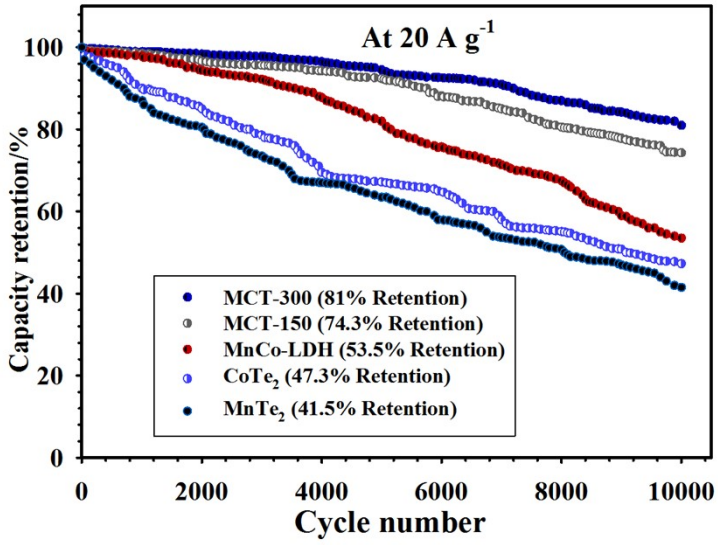

Fig. S9 Longevity of the MCT-300, MCT-150, MnCo-LDH, $CoTe_2$, and $MnTe_2$ electrodes at 20 A g^{-1}.

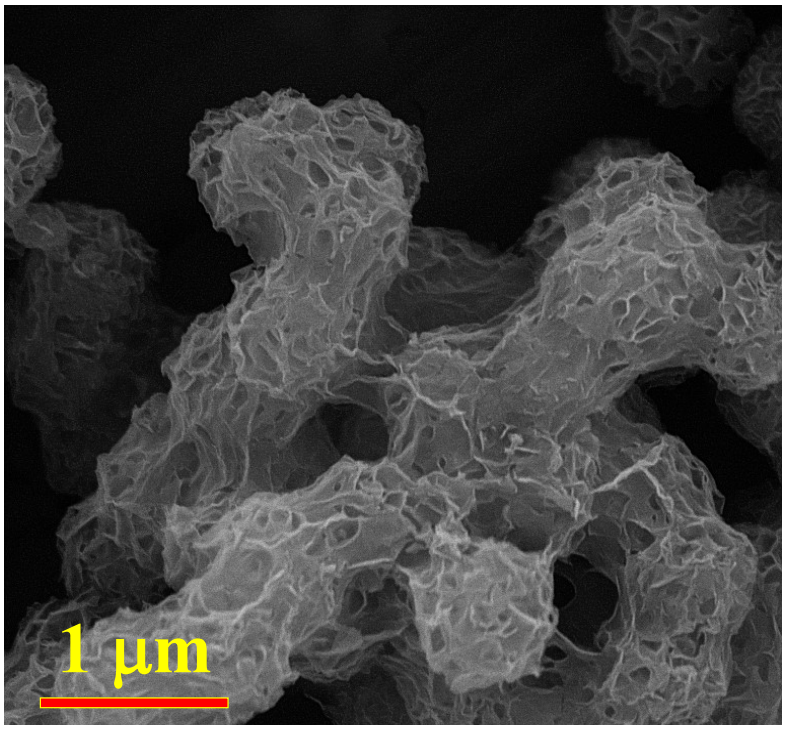

Fig. S10 FESEM image of the MCT-500 after 10000 cycles.

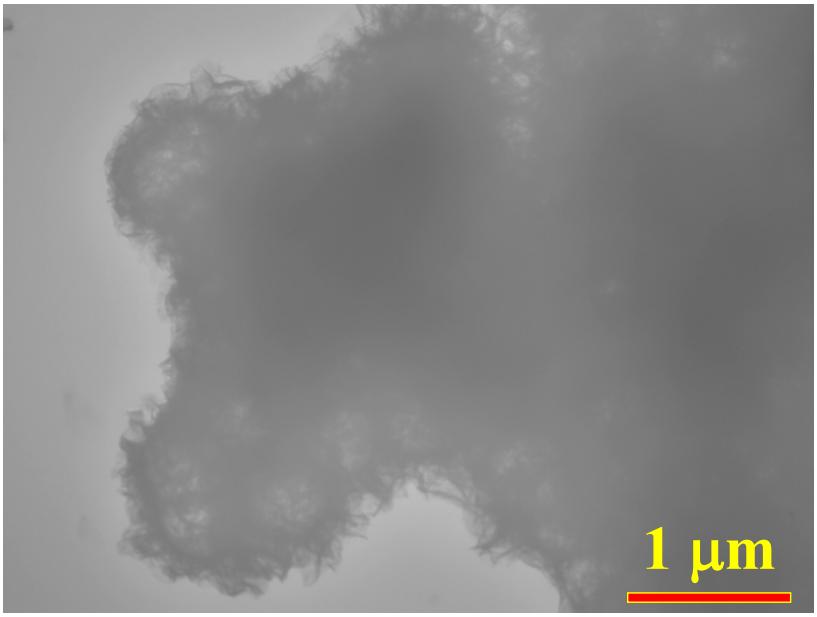

Fig. S11 TEM image of the MCT-500 after 10000 cycles.

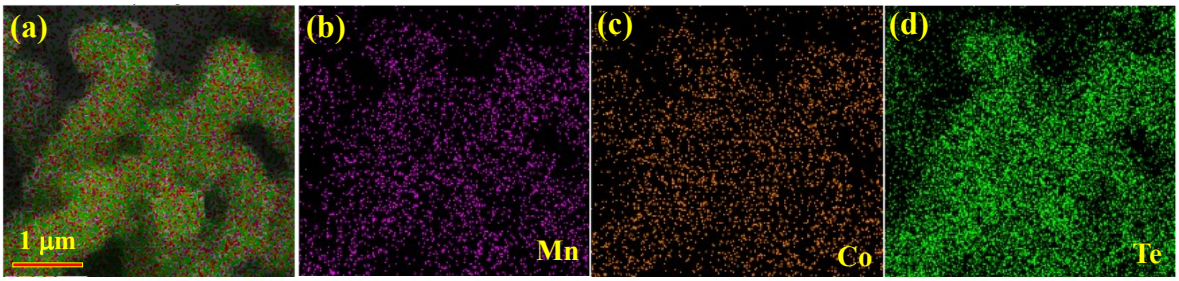

Fig. S12 FESEM mapping images of the MCT-500 after 10000 cycles.

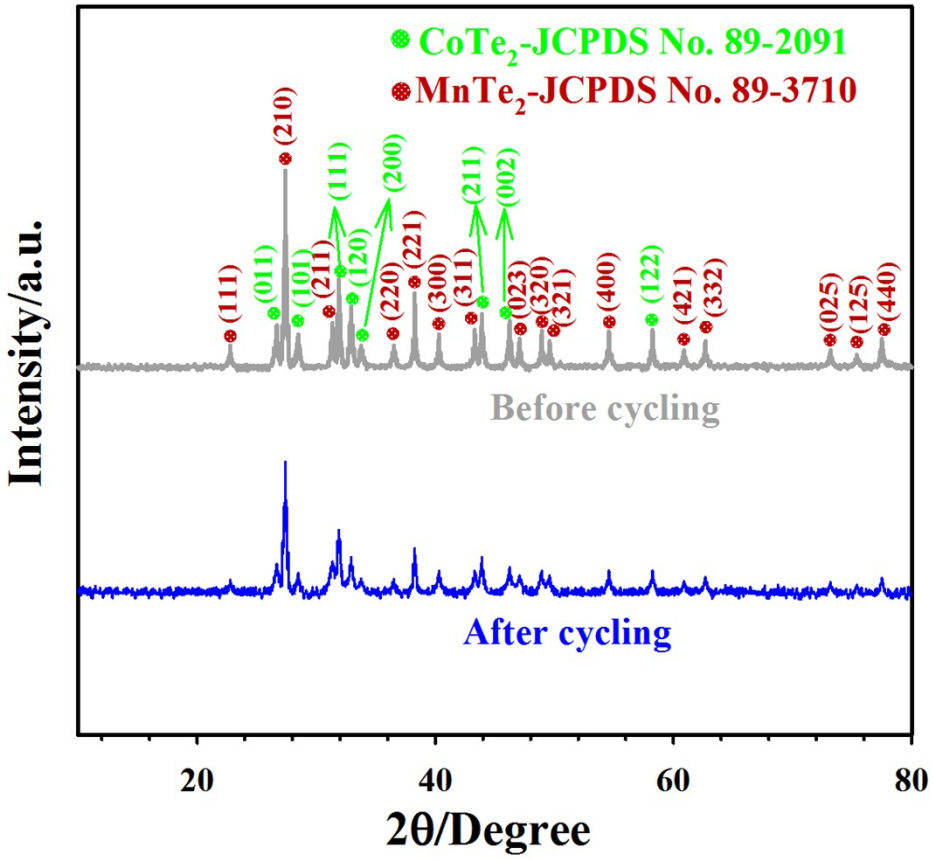

Fig. S13 XRD patterns of the MCT-500 before and after 10000 cycles.

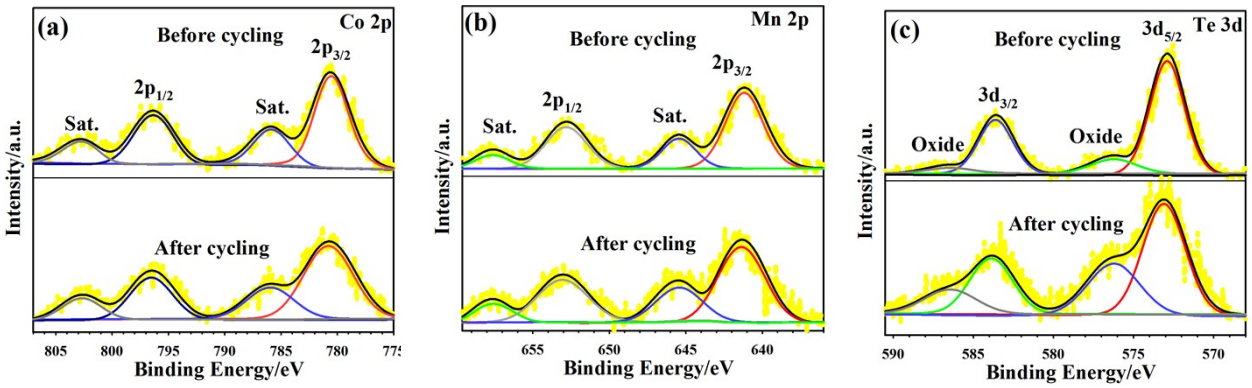

Fig. S14 (a) High-resolution Co 2p XPS patterns of MCT-500 before and after 10000 cycles. (b) High-resolution Mn 2p XPS patterns of MCT-500 before and after 10000 cycles. (c) High-resolution Te 3d XPS patterns of MCT-500 before and after 10000 cycles.

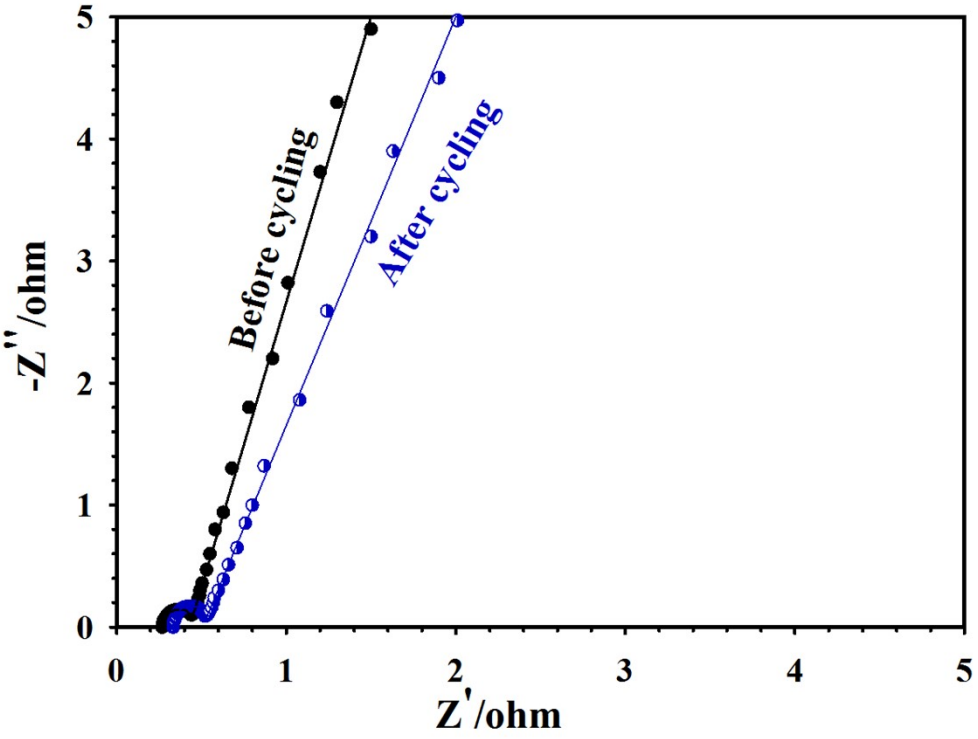

Fig. S15 EIS curves of the MCT-500 before and after 10000 cycles.

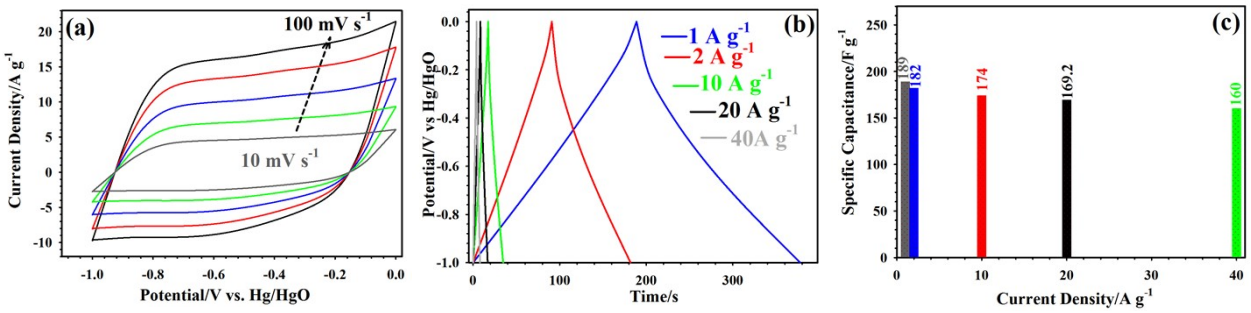

Fig. S16 (a) CV curves of the AC (negative electrode) from 10 to 50 mV s^{-1}. (b) GCD plots of the AC (negative electrode) from 1 to 40 A g^{-1}. (c) Rate capability of the AC electrode (negative electrode).

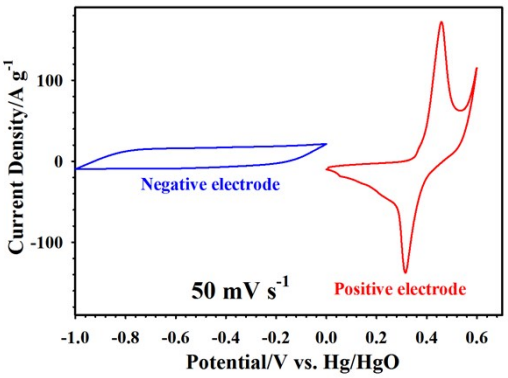

Fig S17 CV plots of AC (negative electrode) and MCT-500 (positive electrode) at 50 mV s^{-1} in three-electrode cell.

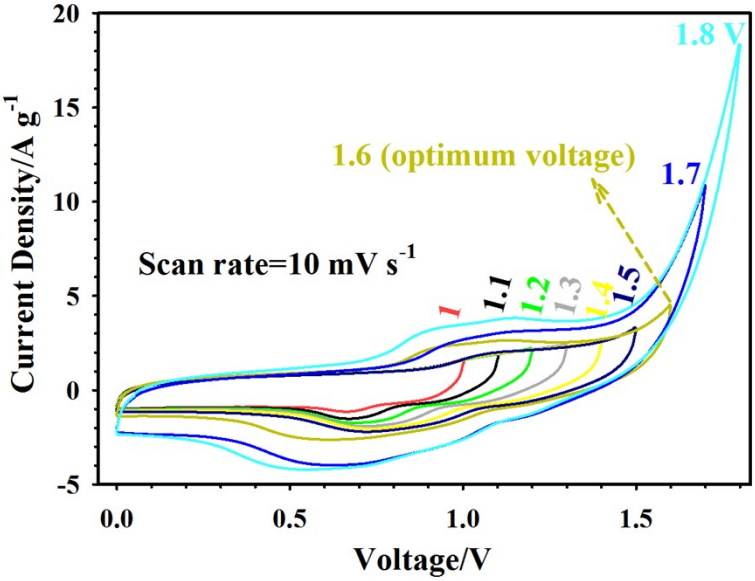

Fig S18 CV plots of the AC//MCT-500 at various potential window at 10 mV s^{-1} from 1.0 to 1.8 V.

Table S1. Comparison of the electrochemical performance of the MCT-500 with other previously reported materials.

Composition	Capacity (C/g)	Cycles, retention	Rate capability	ED (Wh kg^{-1})	Reference
NiTe/ZIF-67	760.5 at 1 A g^{-1}	5000, 93.5% (3 E)	-	43.5	1
NiMnTe	652.5 at 1 A g^{-1}	10000, 82% (3 E)		47.8	2
rGO-CCSe	724 at 1 A g^{-1}	6000, 91.5%	71% at 60 A g^{-1}	57.8	3
CuSe@MnSe	635.32 at 1 A g^{-1}	7000, 91.62%	60.3% at 30 A g^{-1}	19.4	4
CoMnSe@NF	579.6 at 1 A g^{-1}	8000, 91.8%	61.83% at 20 A g^{-1}	55.1	5
3DG/ZnSe–$SnSe_2$	833.36 at 1 A g^{-1}	3000, 90.1%	72.37% at 10 A g^{-1}	32.4	6
CoMnSe@NF	519 at 1 A g^{-1}	5000, 87.07%		35.47	7
N-CQDs/Ni-Co-Se	543.96 at 1 A g^{-1}	5000, 94%	70.1 % at 50 A g^{-1}	41.1	8
(Ni,Co)Se_2/NiCo-LDH	612 at 1 A g^{-1}	3000, 89%	71 % at 20 A g^{-1}	39	9
E_3/MnSe@$Ti_3C_2T_x$-45	612 at 1 A g^{-1}	4000, 90.77%	51.7 % at 10 A g^{-1}	28.68	10
MCT-500	1354 at 1 A g^{-1}	10000, 89.2% (3 E)	68.25% at 40 A g^{-1}	64.88	This study

References

1 K.L. Meghanathan, M. Parthibavarman, V. Sharmila and J.R. Joshua, *J. Energy Storage*, 2023, **72**, 108665.

2 P.-Y. Tai, M. Sakthivel, L.-Y. Lin and K.-C. Ho, *J. Energy Storage*, 2025, **119**, 116362.

3 S.E. Moosavifard, A. Mohammadi, M. Ebrahimnejad Darzi, A. Kariman, M.M. Abdi and G. Karimi, *Chem. Eng. J.*, 2021, **415**, 128662.

4 G. Tang, X. Zhang, B. Tian, P. Guo, J. Liang and W. Wu, *Chem. Eng. J.*, 2023, **471**, 144590.

5 C. Miao, P. Xu, J. Zhao, K. Zhu, K. Cheng, K. Ye, J. Yan, D. Cao, G. Wang and X. Zhang, *ACS Appl. Energy Mater.*, 2019, **2**, 3595–3604.

6 T. Zhao, G. Feng, L. Zhou, X. Wang, X. Li, F. Jiang, H. Li, Y. Liu, Q. Yu, H. Cao, Y. Xu and Y. Zhu, *ACS Appl. Nano Mater.*, 2024, **7**, 13434–13446.

7 A.D. Savariraj, L. Kulandaivel, J.W. Park, P. Sivakumar, R. Manikandan, B.C. Kim and H. Jung, *ACS Appl. Energy Mater.*, 2024, **7**, 735–748.

8 Z. Lu, Z. Hu, L. Xiao, Y. Xie, L. Li, N. Xi, W. Chen, J. Xiao and Y. Zhu, *Chem. Eng. J.*, 2022, **450**, 138347.

9 X. Li, H. Wu, C. Guan, A.M. Elshahawy, Y. Dong, S.J. Pennycook and J. Wang, *Small*, 2019, **15**, 1803895.

10 S. Li, Q. Song, C. Fang, Y. Lu, X. Ding, T. Liu, J. Zhang and F.J. Xu, *Small*, 2025, **21**, 2409130.